China Ocean Eng., Vol. 28, No. 5, pp. 629 – 644

DOI 10.1007/s13344-014-0050-3, ISSN 0890-5487

Consolidation and Creep Behaviors of Two Typical Marine Clays in China*

JIANG Ming-jing (蒋明镜)[a, b, c, 1], LIU Jing-de (刘静德)[c] and YIN Zhen-yu (尹振宇)[d]

[a] *State Key Laboratory of Disaster Reduction in Civil Engineering*, *Tongji University*, *Shanghai 200092*, *China*

[b] *Key Laboratory of Geotechnical and Underground Engineering of Ministry of Education*, *Tongji University*, *Shanghai 200092*, *China*

[c] *Department of Geotechnical Engineering*, *Tongji University*, *Shanghai 200092*, *China*

[d] *Department of Civil Engineering*, *Shanghai Jiao Tong University*, *Shanghai 200240*, *China*

(Received 14 November 2012; received revised form 30 October 2013; accepted 8 January 2014)

ABSTRACT

This paper presents an experimental investigation into the deformation characteristics of two typical marine clays obtained from Dalian and Shanghai, respectively, in China. Three kinds of laboratory tests, i.e. conventional oedometer tests, one-dimensional and triaxial creep tests were carried out. The results obtained from consolidation tests demonstrate linear $e-\log\sigma_v$ relationships for Shanghai clay at normally consolidated state, while partly or even global non-linear relationships for Dalian clay. The compression index C_c for both clays follows the correlation of $C_c=0.009(w_L-10)$ where w_L is the liquid limit of soil. The relationship between $\log k_v$ (k_v is the hydraulic conductivity of soil) and void ratio e is generally linear and the hydraulic conductivity change index C_{kv} can be described by their initial void ratio for both clays. The secondary compressibility of Dalian clay lies in medium to high range and is higher than that of Shanghai clay which lies in the range of low to medium. Furthermore, based on drained triaxial creep tests, the stress-strain-time relationships following Mesri's creep equation have been developed for Dalian and Shanghai clays which can predict the long-term deformation of both clays reasonably well.

Key words: *marine clay*; *compressibility*; *consolidation*; *creep*

1. Introduction

Deposited in a biological, chemical and physical process in saline water (Rajasekaran *et al*., 1998), the marine clays are generally featured by poor strength and high compressibility (Leroueil *et al*., 1992; Li *et al*., 2011; Tanaka *et al*., 2001). Notably, intolerable settlement often occurs to the geotechnical structures resting on the marine sediments even when they are still strong enough. In such case, it is necessary to characterize the compression behaviors of marine clays for predicting the foundation settlement.

The consolidation behaviors of marine clays have been investigated by many authors (Burland, 1990; Jiang *et al*., 1998, 2009; Leroueil *et al*., 1992; Liu and Carter, 2003; Mesri, 1973; Shi and Deng,

* This work was financially supported by China National Funds for Distinguished Young Scientists (Grant No. 51025932), Program for Changjiang Scholars and Innovative Research Team in University (Grant No. IRT1029), Ph. D. Programs Foundation of the Ministry of Education of China (Grant No. 20100072110048) and the National Natural Science Foundation of China (Grant No. 10972158).

1 Corresponding author. E-mail: mingjing.jiang@tongji.edu.cn

2005; Tanaka *et al*., 2001). Based on the experimental data, many theories and constitutive models (Asaoka *et al*., 2000; Ma, 2007; Rouainia and Wood, 2000; Yin *et al*., 2011a) have been proposed to predict the consolidation behavior of soils. Among these attempts, the effective stress concept and the Terzaghi theory have been widely used to estimate the foundation settlement due to consolidation.

The creep properties of marine clays, which characterize their compression behaviors under constant effective stress, play an important role in the long-term stability and settlement of structures established on them. Many authors have experimentally and theoretically investigated the time effects of soft soils from the aspect of their creep behaviors (Leroueil *et al*., 1985; Mesri *et al*., 1981; Singh and Mitchell, 1968; Yin *et al*., 2002, 2010a, 2010b, 2011b; Yin and Hicher, 2008; Yin and Karstunen, 2011; Yin and Wang, 2012). The Mesri model (Mesri *et al*., 1981) and the Singh model (Singh and Mitchell, 1968) are now widely used to predict the stress-strain-time behaviors of clays.

This paper focuses on the deformation behaviors of two marine clays from Dalian and Shanghai in China. Dalian clay is from the seabed where an ongoing offshore reclaimed land rests on. The settlement, especially the long-term settlement, is one of the main concerns in the design of the reclamation. Shanghai clay is the marine clay widely involved in geotechnical engineering in China. In addition, a continuous subsidence at an annual rate of 2−3 mm is reported in this region due to the compaction of marine clay which undermines the performance of various infrastructures. Hence, a better understanding of the compression behaviors of both marine clays is required for predicting the settlements due to consolidation and creep.

In this paper, the deformation behaviors of both marine clays are investigated by performing laboratory tests in which the native sea water and fresh water are used for Dalian and Shanghai clay, respectively. The consolidation behaviors of Dalian and Shanghai marine clays are first studied by means of conventional oedometer tests. Then the creep behaviors of both clays under one- and three-dimensional conditions are investigated. Furthermore, the stress-strain-time relationships for both clays are developed to estimate their creep behaviors.

2. Soils and Testing Programme

2.1 Soils

The investigation in this paper was carried out on the intact samples retrieved from the seabed of Jinzhou Bay, Dalian and the urban area of Shanghai, respectively, as shown in Fig. 1. Tables 1 and 2 present the general geological information and depositional history for the two marine clays. Obviously, the seashore formation can be observed immediately above the fluvial formation due to the rapid sea-level rise from late Pleistocene to early Holocene (ca. 10000−7000 years B. P.) which led to the world wide transgression (Stanley and Warne, 1994). It is the transgression deposition that produces the seashore formation in Dalian and Shanghai. Ever since early Holocene, a regressive succession has occurred in Shanghai due to the seaward migration of the Yangtze delta (Hori *et al*., 2001). Hence, the fluvial yellow silt and silty clay deposit immediately above the marine depositions formed in Shanghai. In contrast, the fluvial depositions above seashore formation are absent in Jinzhou Bay.

The thin wall stationary piston sampler was used to obtain the samples, which were sealed on site

immediately to prevent the loss or gain of moisture. All the samples were then transported to laboratory where they were carefully wire trimmed into specimens with the desirable sizes for testing. All cares should be taken to prevent the soil disturbance in the process of sampling and specimen preparation. Note that the specimen of natural soft clay is often disturbed in laboratory tests due to the sample retrieving, transport and storage, as well as the specimen preparation and installation. The disturbance will reduce the yielding stress or shear strength of the clay. The field tests demonstrate that the in-situ shear strengths of Dalian clay are 32.3 and 156.0 kPa at the depth of 10 and 18 m, respectively. The corresponding shear strength obtained from undrained shear tests in laboratory are 27.7 and 150.0 kPa, respectively. Therefore, the specimens of Dalian clay retrieved from the depths of 10 and 18 m underwent slight disturbance before testing. The physical properties of Dalian and Shanghai clay tested in laboratory are presented in Table 3. The results indicate that the liquid index for both clays decreases with the increasing depth.

Fig. 1. Sampling location of the marine clays studied in this paper.

Table 1 Hydrological geology for Dalian clay

Chronologic	Lithologic characters	Depth (m)	Formation
Holocene	Muddy clay	0−10	Sea shore facies
	Gray mild clay	11−22	
	Silty clay Sand interlayer	22−27	Intermediate facies
	Silty clay Yellow silty clay	27−58	Fluvial facies

Table 2 Hydrological geology for Shanghai clay

Chronologic	Lithologic characters	Depth (m)	Formation
Holocene	Brown yellow mild clay	0−5	Fluvial facies
	Gray muddy clay Clay and sand interlayer Mild clay	5−25	Sea shore facies
Late Pleistocene	Dark green clay	25−35	Fluvial facies
	Yellow silty clay	35−40	
	Green gray silty clay	40−50	Sea shore facies
	Gray mild clay and interlayer sand	50−75	

In order to take into account the influence of salinity of pore water on the compressibility of soils, the native seawater taken from Dalian is used in all the tests on Dalian clay. The salinity concentration

of the seawater is 0.05 g/ml. On the other hand, the fresh water was always used in the tests on Shanghai clay which is now mainly encompassed in groundwater system.

Table 3 Physical properties for the clay used in the investigation

Soil	Depth (m)	Water content w (%)	Void ratio e	Plastic limit w_P (%)	Liquid limit w_L (%)	Liquid index I_L
Dalian clay	9−10	63.90	1.666	20.50	64.30	0.99
	17−18	44.67	1.232	24.46	46.17	0.93
Shanghai clay	5−6	42.17	1.147	22.54	37.23	1.34
	14−15	50.49	1.377	30.79	51.61	0.95

2.2 Testing Programme

Three types of tests were performed on the specimens taken from Dalian and Shanghai.

(1) Conventional oedometer tests were carried out on the two marine clays to characterize the compression behaviors due to consolidation. The hydraulic conductivity can be determined from the testing results. An additional consolidation test was also performed on the specimen of Dalian clay saturated in fresh water to identify the influence of pore water.

(2) One-dimensional creep tests were carried out on the intact specimens of the two marine clays to characterize their creep behaviors under one-dimensional condition.

(3) Drained triaxial creep tests were carried out on the intact specimens of the two clays to characterize their creep behaviors under three-dimensional condition from which the stress-strain-time relationships are determined.

In the present study, the specimens in one- and three-dimensional creep tests were all multi-stage loaded, and the temperature was controlled at 20ºC with a fluctuation of ±1ºC.

3. Conventional Oedometer Tests

The compression behaviors of clays under one-dimensional condition were investigated by conventional oedometer tests which were performed on the double-drained specimens with the height of 20 mm and the diameter of 61.8 mm. The deformation of specimen was measured by a dial gauge with the accuracy of 0.01 mm. In the oedometer tests, the specimens were multi-stage loaded with the pressure increasing from 50 to 1600 kPa. The incremental stress ratio is 1.0. The stress level would not increase until the deformation rate was smaller than 0.01 mm/h. In the oedometer tests on Dalian clay, the fresh and native seawater systems were used to identify the influence of the salinity of pore water on its compression behaviors.

3.1 Compression Behaviors

The compression behaviors of Dalian clay in fresh and sea water are first compared as shown in Fig. 2. Under the vertical stress resulted from the gravity of overlaying soils, natural clays exist with an in-situ void ratio before they are retrieved for the laboratory tests. When they are retrieved for laboratory tests, the in-situ stress is unloaded to the initial stress state of the specimen in laboratory, which depends only on the gravity of the specimen itself. As a result of the unloading, the void ratio of the specimen increases slightly from the in-situ value to initial value (i.e. the initial void ratio) before

testing. In the consolidation tests, the saturated unit weight of the natural clay was about 10 kN/m^3 and the specimens were 2 cm high. The mean vertical effective stress was thus estimated to be 0.1 kPa. Therefore, the initial void ratio is plotted against the stress of 0.1 kPa on the compression curves obtained from laboratory tests, as shown in Figs. 2 and 3. It can be seen that the marine sediments in fresh water exhibit higher compressibility than in sea water system, which indicates that their compression behaviors are generally physic-chemical governed (Mathew and Rao, 1997; Torrance, 1999; Torrance and Pirnat, 1984). Hence, it makes sense to use native sea water for Dalian clay and fresh water for Shanghai clay in the laboratory tests.

Fig. 3 presents the $e-\log\sigma_v$ curves of specimens from Dalian and Shanghai at various depths. The compression and swelling indices are also calculated from the $e-\log\sigma_v$ curves. The $e-\log\sigma_v$ curves for Shanghai marine clay are generally composed of two straight lines indicating the linear relation between the void ratio and $\log\sigma_v$. Such relation for Dalian marine clay, however, is not necessarily linear. The $e-\log\sigma_v$ curve for Dalian clay at the depth of 10 m only consists of one straight line, indicating that it is at the normal consolidated state even at the stress of 50 kPa. In contrast, the $e-\log\sigma_v$ curve for Dalian clay retrieved from the depth of 18 m is global nonlinear, even at the normally consolidated state. When the yielding strength is reached, the $e-\log\sigma_v$ curves for all specimens of the two marine clays are rounded rather than bending sharply, which has been widely reported as the distinct features of compression curves for intact marine clays. It may be caused either by the inherent discontinuity of $e-\log\sigma_v$ relation obtained from odeometer tests, or the disturbance during field sampling and specimen preparation in laboratory. The preconsolidation stresses for both clays, except Dalian clay from the depth of 10 m, are also determined using the Cassagrande method, and the results show that both clays are slightly over-consolidated. Note that the preconsolidation stress determined in this way is somehow objective due to the discontinuity and nonlinearity in the $e-\log\sigma_v$ relation obtained from odeometer tests. In addition, Fig. 3 shows that the Dalian clay retrieved from the depth of 10 m beneath seabed has been in its normal consolidated state under the vertical stress of 50 kPa. This makes it hard to determine the preconsolidation pressure of this clay from its compression curve in Fig. 3. Hence, the corresponding preconsolidation pressure will be not discussed in the following paragraphs.

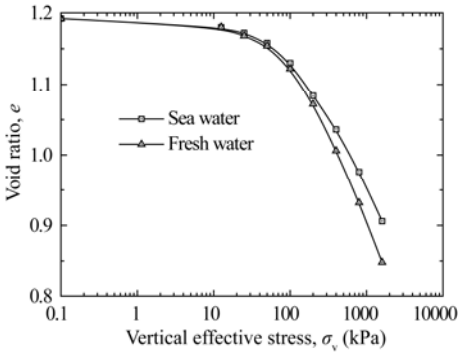

Fig. 2. $e-\log\sigma_v$ curves for marine clay at the depth of 18 m below seabed in fresh and sea water system, respectively.

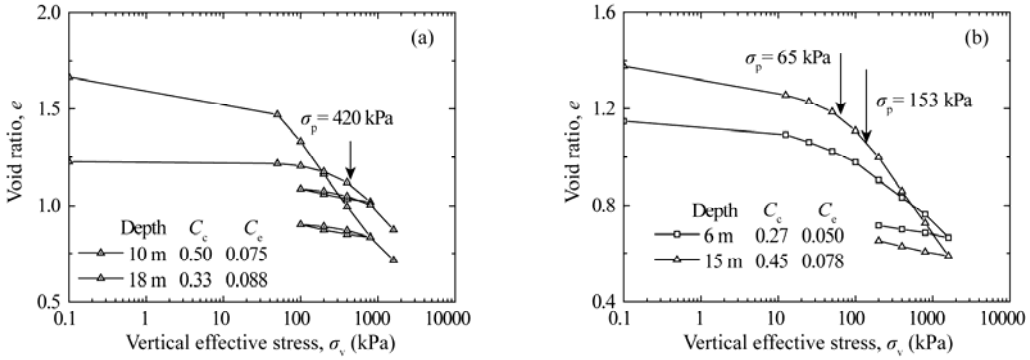

Fig. 3. $e-\log\sigma_v$ curves obtained for (a) Dalian clay and (b) Shanghai clay from odeometer tests.

Owing to the effects of soil structure, the highest compressibility of marine clays are often observed when the initial yielding occurs accompanied by the destructuration, which usually takes place when the consolidation pressure is in the range from $0.75\sigma'_y$ to $2.0\sigma'_y$, σ'_y being the yielding strength (Mesri and Choi, 1984). Fig. 4 presents the variations of compression index against consolidation pressure for Dalian and Shanghai clays. As shown in Fig. 4, the decrease of compression index is only observed for the specimen of Dalian clay at the depth of 10 m. The compression index for other specimens generally increases with the consolidation pressure. This indicates that the structure effects are not very notable for both marine clays.

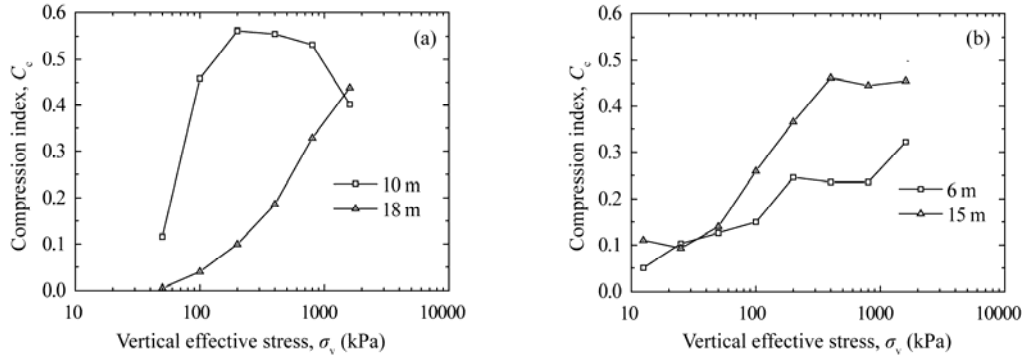

Fig. 4. Relationships between compression index and consolidation pressure for (a) Dalian clay and (b) Shanghai clay.

The compression index C_c of soils is often related to their liquid limit w_L, which is expressed as $C_c = 0.009(w_L - 10)$. This relation can predict the value of C_c for reconstituted specimens and normally consolidated intact specimens for most soils (Tanaka *et al*., 2002). The compression index C_c for Dalian and Shanghai marine clays at normally consolidated state is plotted against w_L as shown in Fig. 5a, which also presents such relationships for several other typical soft clays. It can be seen that both marine clays investigated in this paper follow this correlation due to the fact that the compressibility of soft clays at normally consolidated sate closely associates with the mineral compositions which also determine the liquid limit of the soil.

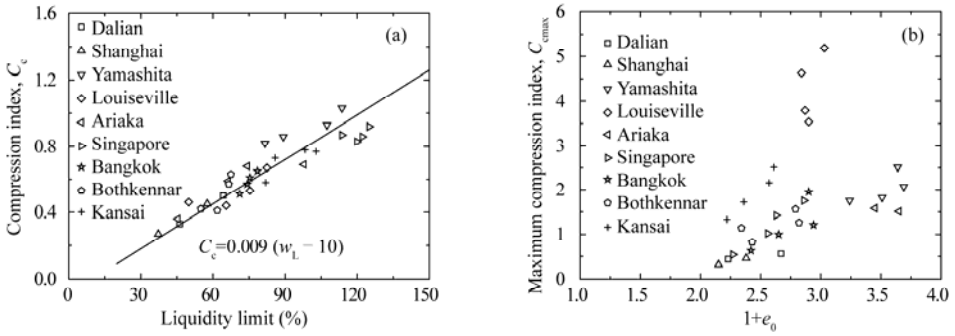

Fig. 5. Compression index for Dalian, Shanghai and several other natural clays.

3.2 Hydraulic Conductivity

The hydraulic conductivity k_v of marine clays can be obtained from the consolidation test using the following formulation:

$$k_v = c_v m_v \gamma_w , \tag{1}$$

where c_v is the coefficient of consolidation, m_v is the coefficient of volume compressibility, and γ_w is the unit weight of water. Eq. (1) comes from the definition of c_v in the Terzaghi's one-dimensional consolidation theory. It is known that there are several fundamental assumptions in Terzaghi's theory: (1) the soil is saturated and homogenous; (2) the soil's compressibility and permeability are constant during the consolidation process; (3) the soil grains and the pore water are incompressible; (4) the flow of pore water are one-dimensional and in accordance with Darcy's law; (5) the deformation of soil is one-dimensional and there is a linear relationship between the void ratio and effective stress. In fact, the variables m_v, k_v and c_v of clay change significantly with the reduction of void ratio during consolidation. In addition, the soil may be regarded as inhomogeneous because c_v reduces faster near the drainage boundaries than in the middle of the specimen during the consolidation. Consequently, Eq. (1) only gives the estimation on the real hydraulic conductivity k_v of the specimen.

The hydraulic conductivity values obtained from laboratory tests are in the range between 1.5×10^{-11} and 5.1×10^{-10} m/s for Dalian clay, and between 1.8×10^{-10} and 5.3×10^{-9} m/s for Shanghai clay. Fig. 6 presents the variation of k_v with the void ratio. Obviously, the relationships between void ratio and $\log k_v$ for both clays are generally linear, which have been observed in the consolidation tests on various clays (Leroueil *et al*., 1992). The hydraulic conductivity has been suggested being predicted by its value at the initial void ratio k_{v0} and the hydraulic conductivity change index C_{k_v} (Leroueil *et al*., 1992), which is the slope of line in Fig. 6. The values of C_{k_v} for Dalian and Shanghai clays and other clays are plotted against the initial void ratio in Fig. 7. The values of C_{k_v} for Dalian clay can be described by $C_{k_v} = 0.35e_0$, which is similar to the relationship for Singapore clay. On the other hand, the values of C_{k_v} for Shanghai clay can be described by $C_{k_v} = 0.52e_0$, which is similar to the relationship for Bothkennar's and other clays. The differences mainly result from the deposition

condition and history of these clays.

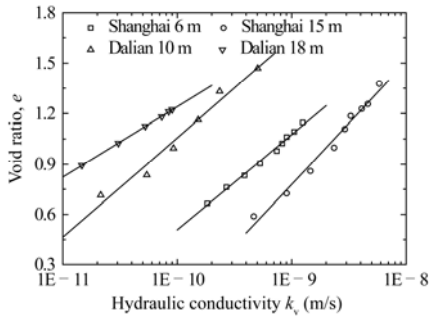

Fig. 6. Hydraulic conductivity for Dalian and Shanghai clays obtained from oedometer tests.

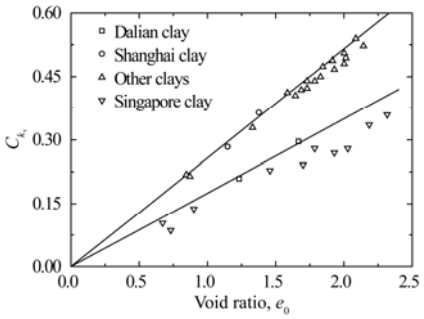

Fig. 7. Relationship between C_{k_v} and e_0 obtained from laboratory tests.

4. One-Dimensional Creep Tests

The one-dimensional creep behaviors of Dalian and Shanghai clays are investigated by performing oedometer creep tests in which the specimen was loaded instantaneously to the desired pressure. The pressure had been then kept constant for a period of time to allow the occurrence of creep. The vertical pressure was increased to the following stage only when the deformation was smaller than 0.01 mm in 24 hours. The pressures applied in the oedometer creep tests were in the range from 50 to 1600 kPa and the incremental stress ratio was 1.0, which were the same as in conventional consolidation tests.

4.1 One-Dimensional Creep Behaviors

Since the $e-\log t$ curves for a given specimen under different pressures are generally similar to each other, only several typical $e-\log t$ curves are presented in Fig. 8 for clarity. It can be seen from Fig. 8 that the $e-\log t$ curves for each specimen at given consolidation pressures are "S" in shape. It indicates that the deformation of specimen can be clearly divided into two stages, i.e. primary and secondary compression stage.

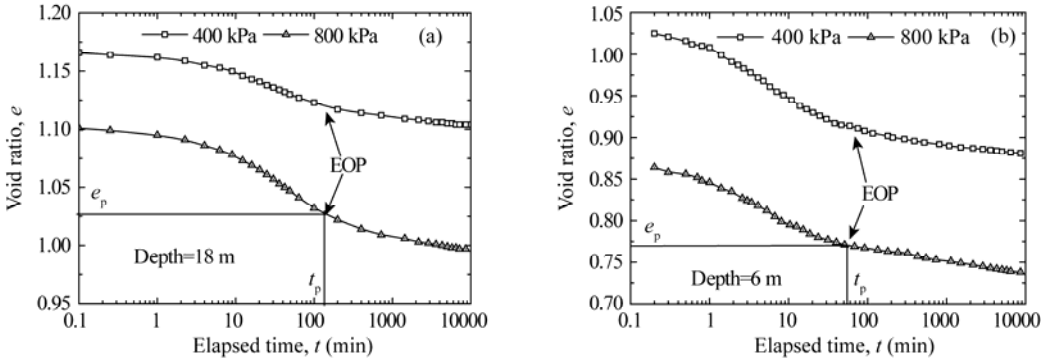

Fig. 8. Typical $e-\log t$ curves for (a) Dalian clay and (b) Shanghai clay.

The Cassagrande method is used to determine the end-of-primary (EOP) e_p and the corresponding time t_p. Obviously, the secondary compression under the constant effective stress can be observed in a rather long duration after the completion of primary consolidation. The duration of the secondary compression generally increases with the increasing effective stress. It is because that the secondary consolidation is closely related to the soil structure alteration (Mesri and Castro, 1987) at particulate level and the diffusion of double-layer (Fang and Gu, 2007), both of which are characterized by stress-dependent and time consuming.

4.2 Secondary Compressibility

The secondary compression index $C_\alpha = \mathrm{d}e / \mathrm{d}\lg t$, the slope of $e - \log t$ relation at the secondary compression stage, is often used to estimate the deformation due to the secondary consolidation. Fig. 9 presents the variations of C_α with the elapsed time. It can be seen from Fig. 9 that the values of C_α for both marine clays decrease with the elapsed time. Such decrease is small at over-consolidated state and becomes dramatic at normally-consolidated state. The secondary compression index will converge to a small value irrespective of consolidation pressure when the creep duration is long enough (about $100\,t_p$ in this paper). The decrease in C_α reflects the attenuation of the secondary compression under one-dimensional drained conditions which comes from the compactness effects with the increasing time. It can also be seen that C_α at EOP for all specimens increases dramatically with consolidation pressure, which is similar to the variation of the compression index C_c.

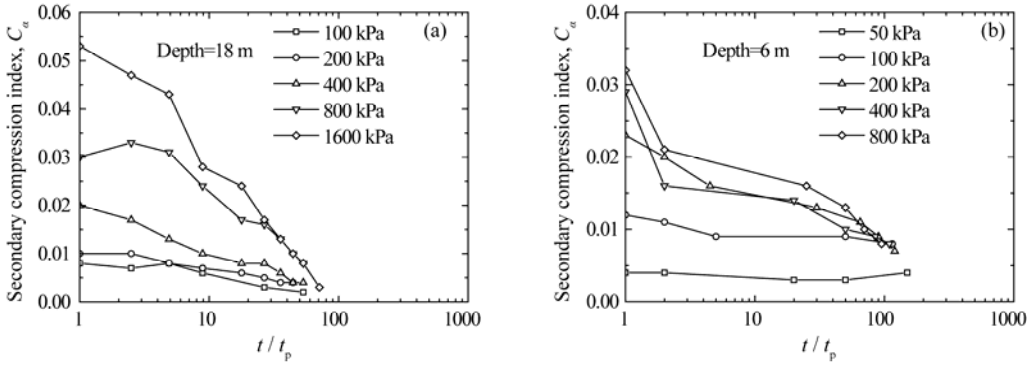

Fig. 9. Variation of the secondary compression index with time for (a) Dalian clay and (b) Shanghai clay under different consolidation pressures.

The C_α / C_c concept of the compressibility proposed by Mesri and Godlewski (Mesri and Castro, 1987) has been widely used to predict the secondary compression behaviors of soft soils. Fig. 10 presents the relation between C_α and C_c for Dalian and Shanghai clays. As shown in Fig. 10, the value of C_α are almost increased linearly with C_c, which have confirmed the validity of the C_α / C_c concept of the compressibility. Moreover, the value of C_α / C_c is 0.043 for Shanghai clay and 0.059 for Dalian clay. According to Terzaghi *et al*. (1996), the values of C_α / C_c for inorganic clay, organic clay and peat clay are in the range of 0.04±0.01, 0.05±0.01 and 0.06±0.01, respectively. Hence,

C_α / C_c for Shanghai clay lies in the range for inorganic clay. On the other hand, C_α / C_c is equivalent to the upper limit for organic clay and lies in the range for peat clay. It implies that Dalian clay exhibits much larger secondary compressibility than Shanghai clay.

The coefficient of secondary compression $\varepsilon_\alpha = C_\alpha / (1+e)$ is another index to measure the secondary compressibility of soils. Fig. 11 presents the relationship between this coefficient and consolidation pressure. According to Fig. 11, the secondary compressibility of Dalian and Shanghai clays increases with the consolidation pressure, confirming the observation made from Fig. 9. The coefficients of the secondary compression for both clays are no more than 0.2 at over-consolidated state. On the other hand, when the consolidation pressure exceeds the yielding stress, the coefficient of the secondary compression for Shanghai clay is in the range of 0.4%−0.8%, while it can be as large as 1.2% for Dalian clay. Mesri has classified the soil in terms of the secondary compressibility, as shown in Table 4. According to Table 4, Shanghai clay exhibits low to medium secondary compressibility, while Dalian clay exhibits high secondary compressibility.

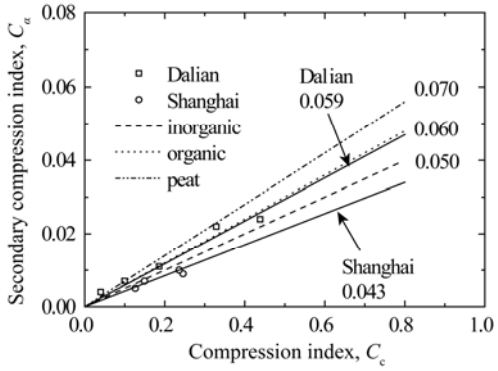

Fig. 10. C_α-C_c relationships for Dalian and Shanghai clays.

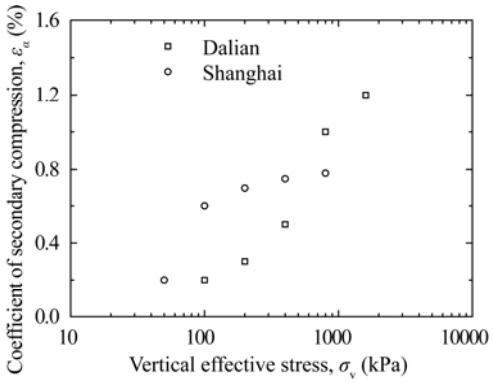

Fig. 11. Coefficients of the secondary compression for Dalian and Shanghai clays.

Table 4 Classification of soils based on the secondary compressibility

ε_α (%)	<0.2	0.4	0.8	1.6	3.2	>6.4
Secondary compressibility	Very low	Low	Medium	High	Very high	Extremely high

5. Drained Triaxial Creep Tests

In civil engineering projects, the soils are often subjected to three-dimensional stresses and the deviator stress will lead to the significant shear deformation. Hence, the creep behaviors of marine clay under three-dimensional condition stress conditions are investigated by performing drained triaxial creep tests on the specimens with the height of 80 mm and the diameter of 39.1 mm. The stress controlled triaxial apparatus was used for the drained triaxial creep tests. The drained condition was achieved by controlling the backpressure at 5 kPa which is low enough to ensure the complete drainage of pore water. During the creep tests, a high accurate transducer was used to measure the deviator stress induced the axial creep deformation.

In the triaxial creep tests, the specimens were first consolidated under the given confining pressure followed by applying the designated deviator stress at the strain rate of 0.01%/min which was slow enough for the dissipation of excessive pore water pressure. All specimens were multi-loaded in the triaxial creep tests. The deformation under a given stress had been observed in a fairly long period to allow the development of creep before the deviator stress was increased to higher level. Note that the creep under drained condition will lead to the structuration effect to the soil, which has strong influence on the mechanical behaviors of the soil. For example, the bulk modulus and the shear strength will increase notably due to the structuration effect. Hence, the incremental deviator stress should be large enough to overcome the structuration effect formed in the previous stage. Otherwise, the deformation in the following stage may be smaller than the real value.

5.1 Triaxial Creep Behaviors

Figs. 12 and 13 show the evolution of the axial strain with elapsed time for Dalian and Shanghai clay, respectively. It can be seen that the creep deformation of all clay samples initiates immediately after the stress has been applied and that the soil creep deformation gradually increases with the elapsed time. However, the creep strain rate decreases with the elapsed time and thus the soil deformation will eventually stabilize at a certain value after a period of creep. It is found that the shear failure of specimens is always caused by loading rather than creep, which differs largely from the failure modes in undrained triaxial creep tests. Such differences can be accounted for by the volumetric changes in the testing. As shown in Figs. 14 and 15, the volumetric strain increases quickly at the beginning of the creep tests, while the strain rate continues to decrease with the elapsed time. It indicates that the pore water of specimens will gradually dissipate during the drained triaxial creep tests, which will lead to the compaction of the soil skeleton. Hence, the soil usually tends to get harder due to creep and failure hardly occurs in the creep stage under drained condition. It is worth pointing out that the creep deformation under drained condition is not as notable as that under the undrained condition because the consolidation of soil could also weaken or even eliminate creep effects of soil at a constant stress.

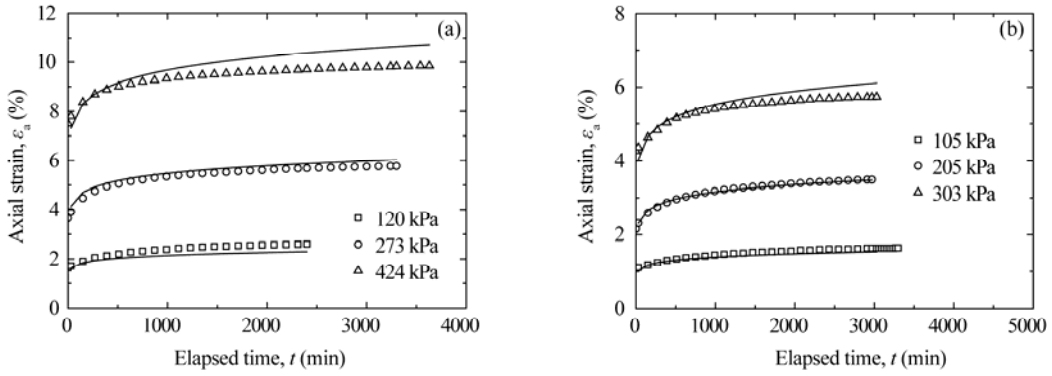

Fig. 12. Axial strain−time curves ($\sigma_3 = 400$ kPa) for Dalian clay at the depth: (a) 10 m and (b) 18 m.

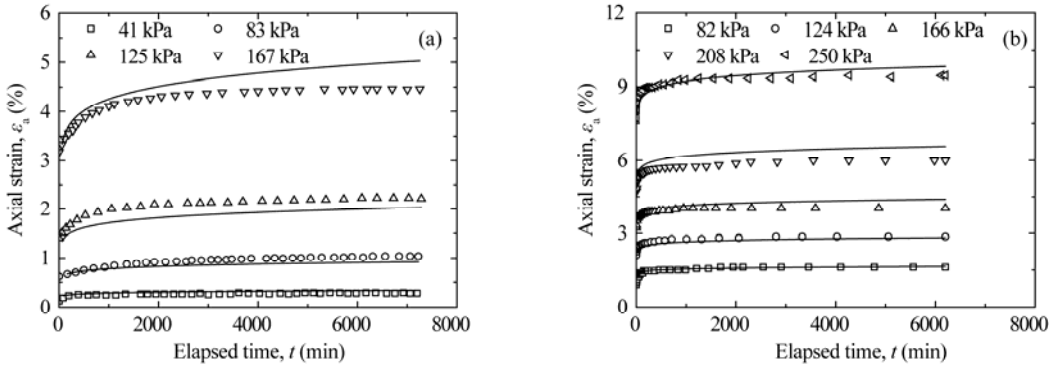

Fig. 13. Axial strain−time curves ($\sigma_3 = 100$ kPa) for Shanghai clay at the depth: (a) 6 m and (b) 15 m.

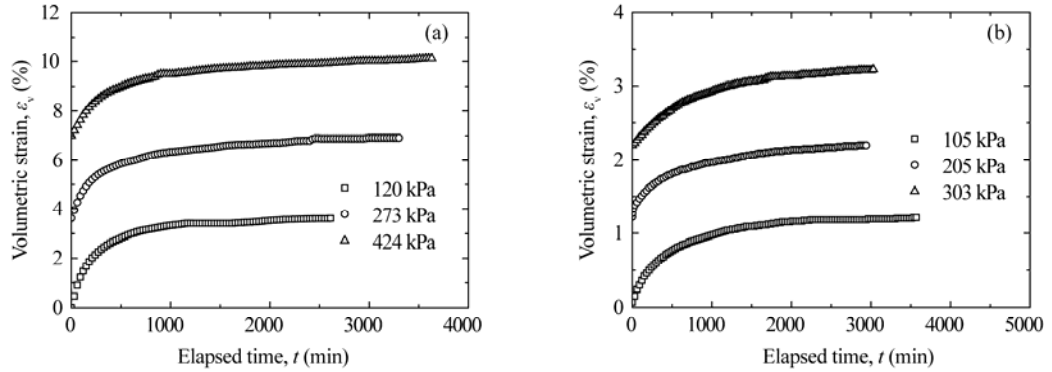

Fig. 14. Volumetric strain−time curves ($\sigma_3 = 400$ kPa) for Dalian clay at the depth: (a) 10 m and (b) 18 m.

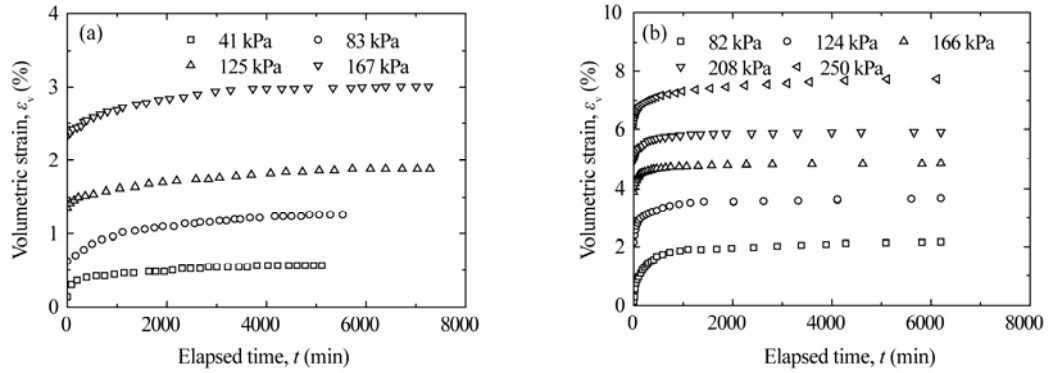

Fig. 15. Volumetric strain−time curves ($\sigma_3 = 100$ kPa) for Shanghai clay at the depth: (a) 6 m and (b) 15 m.

5.2 Stress-Strain-Time Relationship

It is important to develop the stress-strain-time relationship for predicting the long-term deformation of soil. Based on experimental results, Mesri *et al*. (1981) proposed such a relationship expressed as:

$$\varepsilon = \frac{2}{\left(E_u / S_u\right)_1} \frac{D_1}{1-\left(R_f\right)_1 D_1} \left(\frac{t}{t_1}\right)^{\lambda}, \tag{2}$$

where E_u is the initial tangent elasticity modulus, S_u is the shear strength at failure, R_f is the stress ratio at failure, t_1 is the reference time with respect to which the creep deformation of soil is calculated, D_1 is the stress level at which the creep is observed, and λ is the parameter reflecting the time-dependent of soil deformation and can be determined by fitting the experiment results. Obviously, the Mesri creep equation adopts two assumptions: (1) the strain of soil at constant stress level increases exponentially with time; (2) soil hardens with the increasing strain in a hyperbolic way.

It can be seen from Figs. 16 and 17 that $\log\varepsilon - \log t$ curves for each specimen are in general at a family of parallel lines with the slope of λ. This observation is in good agreement with the assumption about the strain-time relation of soil in the Mesri creep equation. In Fig. 18, the curves of $\frac{\varepsilon_a}{D_1} - \varepsilon_a$ are almost linear, indicating the hyperbolic relation between stress and strain. It can be concluded from the above observations that the stress-strain-time relationships for Dalian and Shanghai clay can be modeled using the Mesri creep equation. The parameters of the Mesri creep equation for Dalian and Shanghai clays are summarized in Table 5. The stress-strain-time relationships can be expressed as follows:

Dalian clay:

$$\varepsilon = 7.832\frac{D_1}{1-0.378D_1}\left(\frac{t}{t_1}\right)^{0.080} \qquad \text{depth} = 10\ \text{m}; \tag{3}$$

$$\varepsilon = 3.663\frac{D_1}{1-0.469D_1}\left(\frac{t}{t_1}\right)^{0.090} \qquad \text{depth} = 18\ \text{m}. \tag{4}$$

Shanghai clay:

$$\varepsilon = 1.054\frac{D_1}{1-0.968D_1}\left(\frac{t}{t_1}\right)^{0.084} \qquad \text{depth} = 6\ \text{m}; \tag{5}$$

$$\varepsilon = 4.780\frac{D_1}{1-0.789D_1}\left(\frac{t}{t_1}\right)^{0.034} \qquad \text{depth} = 15\ \text{m}. \tag{6}$$

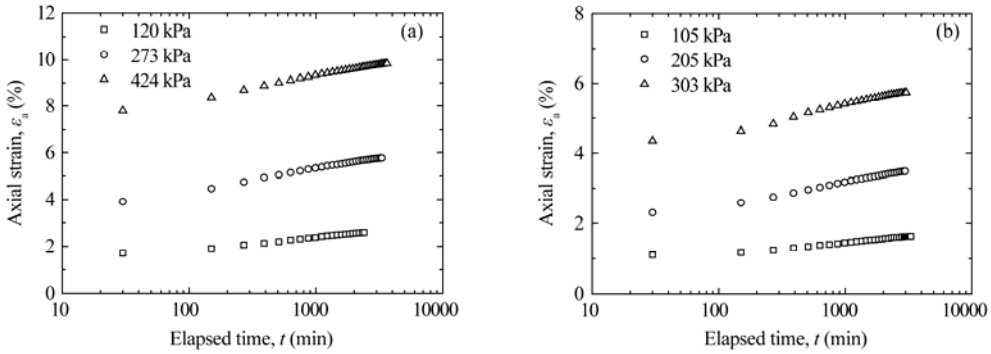

Fig. 16. Axial strain−time curves ($\sigma_3 = 400$ kPa) for Dalian clay at the depth: (a) 10 m and (b) 18 m in log−log coordinate system.

The solid lines in Figs. 12 and 13 are calculated from the above equations. It can be seen that the fitting equations are generally in good accordance with the experimental results.

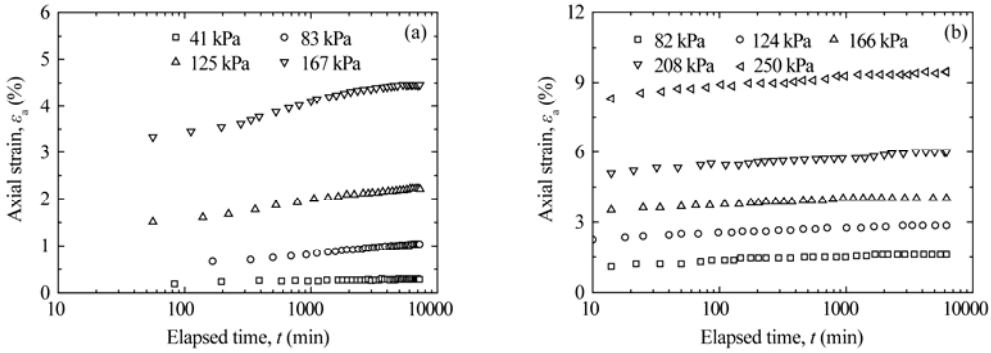

Fig. 17. Axial strain−time curves ($\sigma_3 = 100$ kPa) for Shanghai clay at the depth: (a) 6 m and (b) 15 m in log−log coordinate system.

Table 5 Parameters of the Mesri creep equation for Dalian and Shanghai clays

Clay	Depth (m)	$\left(\frac{2}{E_u/S_u}\right)_1$	$(R_f)_1$	λ					$\bar{\lambda}$
Dalian	9−10	7.832	0.378	0.108	0.082	0.050	−	−	0.080
	17−18	3.663	0.469	0.103	0.098	0.068	−	−	0.090
Shanghai	7−8	1.054	0.968	0.071	0.121	0.081	0.063	−	0.084
	13−14	4.780	0.789	0.062	0.035	0.025	0.027	0.020	0.034

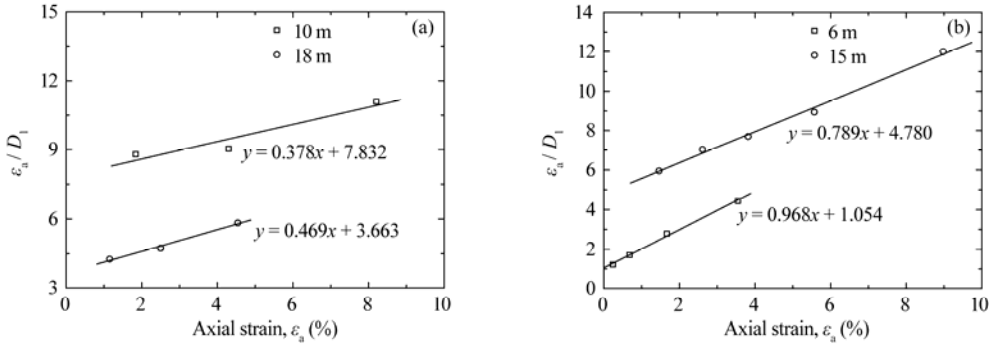

Fig. 18. Relationships of $\frac{\varepsilon_a}{D_1} - \varepsilon_a$ for (a) Dalian clay and (b) Shanghai clay.

6. Conclusions

In this paper, the compressibility of Dalian and Shanghai clays has been studied in laboratory from two aspects: consolidation related to excess pore water dissipation, and creep related to the viscosity of soils. The compression behaviors associated with consolidation were investigated by oedometer tests. On the other hand, the creep behaviors associated with time effects were carefully studied by one-dimensional creep tests and drained triaxial creep tests. Based on all experimental results, the following conclusion can be made:

(1) Compressibility of clays obtained from oedometer tests in fresh water system is found higher than that in saline water system. This observation demonstrates that the clay compressibility is strongly influenced by pore water system due to cation exchange which should be taken into account in the laboratory tests.

(2) At normally consolidated state, the compression curve is linear for Shanghai clay and curved for Dalian clay. The relation between compression index and consolidation pressure implies the rise of compressibility with the increasing pressure. The compression index C_c of both clays can be predicted using the correlation of $C_c = 0.009(w_L - 10)$. The value of $\log k_v$ decreases linearly with the decreasing void ratio by the hydraulic conductivity change index C_{k_v}.

(3) The secondary compression of both Dalian and Shanghai clays can be clearly observed in the oedometer creep tests. Shanghai clay exhibits low to medium secondary compressibility, while Dalian clay exhibits medium to high secondary compressibility, according to the coefficient of secondary compression. The secondary compression index of both marine clays is directly related to the corresponding compression index.

(4) Under drained condition, the creep strain rate of specimens in triaxial creep tests attenuates to a very small level with the increasing time. In addition, the dissipation of pore water will lead to the structuration effects and thus the shear failure would hardly occur due to creep. The results demonstrate the linear $\log\varepsilon - \log t$ relationship, and the hyperbolic stress-strain relationships for both clays. The stress-strain-time relationships for Dalian and Shanghai clays were developed based on the Mesri's creep equation, and the relationship can predict the secondary compression behaviors of both clays under drained condition.

References

Asaoka, A., Nakano, M., Noda, T. and Kaneda, K., 2000. Delayed compression/consolidation of natural clay due to degradation of soil structure, *Soils Found*., **40**(3): 75−85.

Burland, J. B., 1990. On the compressibility and shear strength of natural clays, *Géotechnique*, **40**(3): 329−378.

Fang, Y. G. and Gu, R. G., 2007. Experiment study on the effects of adsorbed water on rheological characteristics of soft clayey soil, *Sci. Technol. Eng*., **7**(1): 73−78. (in Chinese)

Hori, K., Saito, Y., Zhao, Q., Cheng, X., Wang, P., Sato, Y. and Li, C., 2001. Sedimentary facies and Holocene progradation rates of the Changjiang (Yangtze) delta, China, *Geomorphology*, **41**(2): 233−248.

Jiang, M. J., Hongo, T., Fukuda, M., Adachi, T., Oka, F., Shen, Z. J. and Xing, S. Y., 1998. Pre-failure behavior of deep-situated Osaka clay, *China Ocean Eng*., **12**(4): 453−465.

Jiang, M. J., Peng, L. C., Zhu, H. H., Lin, Y. X. and Huang, L. J., 2009. Macro- and micro- properties of two natural marine clays in China, *China Ocean Eng*., **23**(2): 329−344.

Leroueil, S., Kabbaj, M., Tavenas, F. and Bouchard, R., 1985. Stress-strain-strain rate relation for the compressibility of natural sensitive clays, *Géotechnique*, **35**(2): 159−180.

Leroueil, S., Lerat, P., Hight, D. W. and Powell, J. J. M., 1992. Hydraulic conductivity of a recent estuarine silty clay at Bothkennar, *Géotechnique*, **42**(2): 275−288.

Li, L. L., Dan, H. B. and Wang, L. Z., 2011. Undrained behavior of natural marine clay under cyclic loading, *Ocean Eng*., **38**(16): 1792−1805.

Liu, M. D. and Carter, J. P., 2003. Volumetric deformation of natural clays, *Int. J. Geomech*., **3**(2): 236−252.

Ma, D., 2007. A hypoplastic constitutive model for clays with meta-stable structure, *Can. Geotech. J*., **44**(3): 363−375.

Mathew, P. K. and Rao, S. N., 1997. Influence of cations on compressibility behavior of a marine clay, *J. Geotech*.

Geoenviron. *Eng*., **123**(11): 1071−1073.

Mesri, G. and Castro, A., 1987. C_a/C_c concept and K_0 during secondary compression, *J. Geotech. Eng*., **113**(3): 230−247.

Mesri, G. and Choi, Y. K., 1984. Discussion of "Time effects on the stress-strain behaviours of natural soft clays", *Géotechnique*, **34**(3): 439−442.

Mesri, G., Rokhsar, A. and Bohor, B. F., 1975. Composition and compressibility of typical samples of Mexico city clay, *Géotechnique*, **25**(3): 527−554.

Mesri, G., Febres-Cordero, E., Shields, D. R. and Castro, A., 1981. Shear stress-strain-time behaviour of clays, *Géotechnique*, **31**(4): 537−552.

Rajasekaran, G., Murali, K. and Srinivasaraghavan, R., 1998. Microfabric, chemical and mineralogical study of Indian marine clays, *Ocean Eng*., **26**(5): 463−483.

Rouainia, M., and Wood, D. M., 2000. A kinematic hardening constitutive model for natural clays with loss of structure, *Géotechnique*, **50**(2): 153−164.

Shi, M. L. and Deng, X. J., 2005. On physical and mechanical behavior of natural marine intermediate deposits, *China Ocean Eng*., **19**(1): 111−119.

Singh, A. and Mitchell, J., 1968. General stress-strain-time function for soils, *J. Soil Mech*. *Found*., **94**(1): 21−46.

Stanley, D. J. and Warne, A. G., 1994. Worldwide initiation of Holocene marine deltas by deceleration of sea-level rise, *Science*, **265**(5169): 228−231.

Tanaka, H., Locat, J., Shibuya, S., Soon, T. T. and Shiwakoti, D. R., 2001. Characterization of Singapore, Bangkok, and Ariake clays, *Can. Geotech. J*., **38**(2): 378−400.

Tanaka, H., Ritoh, F. and Omukai, N., 2002. *Geotechnical Properties of Clay Deposits of the Osaka Basin*, International Workshop on Characteriatizon and Engineering Properties, Taylor & Francis, Singapore.

Terzaghi, K., Peck, R. B. and Mesri, G., 1996. *Soil Mechanics in Engineering Practice*, John Wiley and Sons Publication.

Torrance, J. K., 1999. Physical, chemical and mineralogical influences on the rheology of remoulded low-activity sensitive marine clay, *Appl. Clay Sci*., **14**(4): 199−223.

Torrance, J. K. and Pirnat, M., 1984. Effect of pH on the rheology of marine clay from the site of the South Nation river, Canada, landslide of 1971, *Clay*. *Clay Miner*., **32**(5): 384−390.

Yin, J. H., Zhu, J. G. and Graham, J., 2002. A new elastic viscoplastic model for time-dependent behaviour of normally and overconsolidated clays: Theory and verification, *Can. Geotech. J*., **39**(1): 157−173.

Yin, Z. Y. and Hicher, P. Y., 2008. Identifying parameters controlling soil delayed behaviour from laboratory and in situ pressuremeter testing, *Int. J. Numer. Anal. Meth. Geomech*., **32**(12): 1515−1535.

Yin, Z. Y. and Karstunen, M., 2011. Modelling strain-rate-dependency of natural soft clays combined with anisotropy and destructuration, *Acta. Mech. Solida. Sin*., **24**(3): 216−230.

Yin, Z. Y. and Wang, J. H., 2012. A one-dimensional strain-rate based model for soft structured clays, *Sci*. *China Ser*. *E*, **55**(1): 90−100.

Yin, Z. Y., Chang, C. S., Karstunen, M. and Hicher, P. Y., 2010a. An anisotropic elastic viscoplastic model for soft soils, *Int. J. Solids Struct*., **47**(5): 665−677.

Yin, Z. Y., Hattab, M. and Hicher, P. Y., 2011b. Multiscale modeling of a sensitive marine clay, *Int. J. Numer. Anal. Meth. Geomech*., **35**(15): 1682−1702.

Yin, Z. Y., Karstunen, M. and Hicher, P. Y., 2010b. Evaluation of the influence of elasto-viscoplastic scaling functions on modelling time-dependent behaviour of natural clays, *Soils Found*., **50**(2): 203−214.

Yin, Z. Y., Karstunen, M., Chang, C. S., Koskinen, M. and Lojander, M., 2011a. Modeling time-dependent behavior of soft sensitive clay, *J. Geotech. Geoenviron. Eng*., **137**(11): 1103−1113.